X-Ray Absorption Spectroscopy of Iron-(II) and -(III) Basket-handle Porphyrins†

Christophe Cartier,[a] Michel Momenteau,*[,b] Elizabeth Dartyge,[a] Alain Fontaine,[a] Gérard Tourillon,[a] Alain Michalowicz[a,c] and Michel Verdaguer*[,a,d]

[a] *Laboratoire d'Utilisation du Rayonnement Electromagnétique (C.N.R.S., C.E.A., M.E.N.), Université de Paris-Sud, 91405 Orsay, France*

[b] *Institut Curie, Section Biologie, Université de Paris-Sud, 91405 Orsay, France*

[c] *Laboratoire de Physico-chimie Structurale, Université de Paris-Val de Marne, 94000 Créteil, France*

[d] *Laboratoire de Chimie des Métaux de Transition, U.A. C.N.R.S. 419, Université P. et M. Curie, 75252 Paris, France*

X-Ray absorption near-edge structure and extended X-ray absorption fine structure spectroscopies have been used to characterize iron basket-handle porphyrins in various co-ordinations, stereochemistries and oxidation states. Attention is paid to the square-planar iron(II) complexes, a dioxygen adduct of Fe^{II} and a hydroxyiron(III) complex. The results are consistent with a $Fe^{II}(O_2)$ rather than a $Fe^{III}(O_2^-)$ formulation for the dioxygen adduct. A Fe–O distance of 1.94 Å was found in the hydroxo complex. The kinetics of oxidation of a dioxygen form to the hydroxo complex has been studied using a dispersive-mode X-ray absorption spectrometer (half-life ≈ 6 min).

During the last ten years several types of superstructured iron porphyrins have been designed in order to mimic the micro-environment of the active sites and the characteristics of the metallic centre, stereochemistry and co-ordination number, oxidation and spin states, which are closely related to the biological functions of haemoproteins.[1] Another important purpose of such an endeavour is to gain fundamental understanding of the behaviour of the synthetic materials, which are interesting by themselves, since they present a large span of chemical and physical properties: flexible co-ordination chemistry on either side of the metallic ion and versatile reactivity in binding dioxygen, carbon monoxide and other ligands. In particular, they provide well characterized compounds, unavailable by any other way, to check theoretical and physical methods and models.

Among such compounds, the so-called basket-handle porphyrins, in cross-*trans* configuration, appear very attractive.[2] These compounds present steric effects on both faces of the porphyrin ring thanks to basket-handle chains linking two opposite phenyl groups of 5,10,15,20-tetraphenylporphyrin (H_2tpp) by ether or secondary amide groups. The length, as well as the chemical nature, of the handle can be varied to tune the size and the polarity of the pockets and also to change the co-ordination, and the spin state of the central metal ion. Their iron(II) complexes are therefore protected against rapid and irreversible oxidation by dioxygen to μ-oxo dimers. The presence of an additional nitrogen base, imidazole or pyridine, hung on to one of the two handles, provided a strict axial five-co-ordination of the central ion and a better stabilization of the dioxygen adduct. Thus, these structures occur as characterized square-planar, square-pyramidal or octahedral complexes, which leads to typical, well differentiated, X-ray absorption near edge structure (XANES) spectra.

Two problems are of particular interest. (*i*) The nature of the oxidation state in the $[Fe^{II}(O_2)L]$ adduct (L = dianion of basket-handle porphyrin). These systems have been described either as $Fe^{II}O_2$ by Pauling,[3] corresponding to the combination of molecular dioxygen with iron(II), without change of the valency of the metallic ion, or following Weiss's hypothesis[4] as $Fe^{III}(O_2^-)$, in which the bonding of the dioxygen involves an electron-transfer process. The $Fe–O_2$ bond description cannot be reduced so simply since the electronic distribution is governed by σ as well as π overlaps[5] and it is not surprising that different techniques have given seemingly contradictory results.[6] (*ii*) The second question is structural in nature: what is the Fe–O distance in the oxidized Fe^{III}–OH form? No precise answer is available, due to the lack of suitable compounds: with simple or single hindered iron porphyrins hydroxy complexes are quickly converted into the corresponding μ-oxo dimers. The appearance of hindered porphyrins has stimulated kinetic[7] and electrochemical[8] studies of such $Fe^{III}(OH^-)$ porphyrins.[9] Unfortunately, no molecular and crystal structures of such compounds have been reported.

X-Ray absorption spectroscopy can probe the relationships between stereochemistry, oxidation and spin states of iron porphyrins.

It is more and more widely used with the availability of intense, tunable, polarized and well collimated X-ray sources.[10] The photoelectric transition transfers the photon energy $h\nu$ to a core electron which becomes a photoelectron in the final state [equation (1)] where μ is the transition moment $\langle i|$ and $\langle f|$ are

$$\mu \propto \sum_{i,f} |\langle i|e\,Er|f\rangle|^2\,\delta\,(E_f - E_i - h\nu) \qquad (1)$$

the ground- and excited-state wavefunctions respectively, E is the electric field vector, e is the electron, δ is a Dirac function and r is the position vector. Reduced to the dipolar approximation, this formalism assigns E_i to the binding energy of the core electron (7112.0 eV in pure metallic iron), and E_f is the energy of the final state.

In the high-energy range (>50–100 eV above the edge), EXAFS (extended X-ray absorption fine structure)[11] describes

† *Non-SI unit employed:* eV ≈ 1.60 × 10^{-19} J.

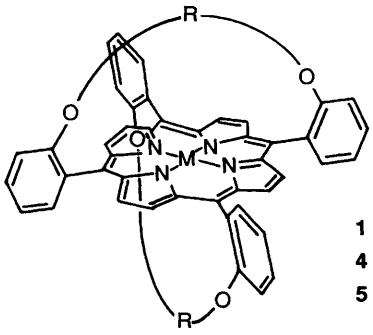

	M	R
1	Fe^{II}	$(CH_2)_{12}$
4	$Fe^{III}(OH)$	$(CH_2)_{12}$
5	$Fe^{III}Cl$	$p\text{-}C_6H_4[(CH_2)_4]_2$

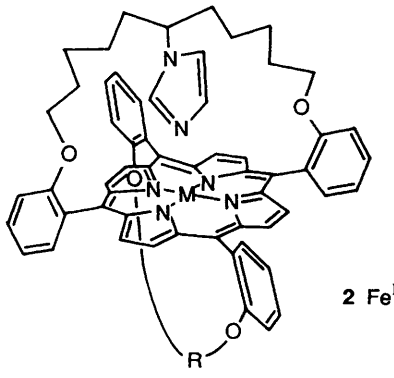

2 Fe^{II} $(CH_2)_{12}$

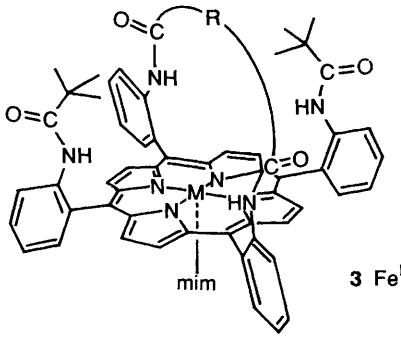

3 $Fe^{II}(O_2)$ $(CH_2)_{12}$

the final state, within the scattering formalism, as the mere superposition of the outgoing wave and the wavelets back-scattered once by the nearest neighbours. The EXAFS wiggles arise from the change in the optical path ($2kR_j$), where k is wave vector associated with the photoelectron at a given kinetic energy and R_j is the distance between the neighbouring atom j and the absorbing atom.

The low-energy range is known as XANES.[12] A unified interpretation is still awaited but it complements the EXAFS results in giving insights into the electronic structure of the absorber (by the analysis of the transitions towards bound states) and into the stereochemistry of the surrounding cluster (using the transitions of the bound states, the continuum resonances and the multiple-scattering features when present). The accessible final states are those of an ion where a core hole has been created followed by a quasi-instantaneous electron shell relaxation: X-ray absorption spectroscopy probes the final states as they exist after a core hole creation and relaxation.

Both EXAFS and XANES have been applied to synthetic tetrapyrrolic macrocycles[13] and to haemoproteins[14] in particular to carbonyl myoglobin, where a polarized single-crystal study was published.[15a] The use of beam polarization with orientated single crystals is growing and gives invaluable information about the nature of the edge transitions.[15b-e]

We report here X-ray absorption spectra of iron basket-handle porphyrins, obtained both in the solid state and in solution. The structural changes of the iron centre during oxidation under a dioxygen atmosphere have been followed *in situ* by time-resolved dispersive X-ray absorption spectroscopy,[16,17] and we report here preliminary results.[18]

Experimental

Sample Preparation.—All solvents and reagents were purchased commercially. The free-base porphyrins used to obtain the iron derivatives investigated were synthesised as previously described.[2] Iron(III) complexes were synthesised in dimethylformamide by using anhydrous iron(II) chloride and purified as described.[2c] Chloro- and hydroxo-iron(III) derivatives were generated by shaking a toluene solution of the metalloporphyrin with aqueous sodium chloride and sodium carbonate, respectively. Reduction to iron(II) complexes was performed in a mixture of water and toluene. Distilled water containing sodium dithionite and a toluene solution of the metalloporphyrin (0.01 mol dm^{-3}) were vigorously stirred under argon for 10 min. After separation of the two phases, the organic layer was transferred under argon to 1 cm thick aluminium cells closed by transparent Kapton windows, through a latex septum, *via* a stainless-steel tube. They were left under an argon atmosphere ($\approx$15–30 min) until recording of the spectrum. The 1-methylimidazole (mim) derivative of Fe^{II} was obtained by addition of the axial base to a 0.1 mol dm^{-3} toluene solution of the metalloporphyrin. Dioxygen adducts were obtained by bubbling pure dioxygen into the corresponding cells directly set in the beam. The cell was equipped with an automatic electromagnetic valve and with a magnetic microbar. The solid iron(III) samples were precipitated from the corresponding solutions by addition of pure heptane, in a metallic glove-box under argon. They were prepared for X-ray absorption measurements as finely ground powders, uniformly dispersed between two X-ray transparent adhesive tapes. The mass employed was such as to avoid too thick samples and saturation effects.

Data are presented for the compounds **1** (square planar), **2** (square pyramidal), **3** (dioxygen adduct), **4** (supposed square pyramidal), **5** (square pyramidal), the crystal structure of which has been determined,[19] and $[\{Fe(tpp)\}_2O]$ **6** prepared following the method described by Cohen.[20a]

EXAFS and XANES Measurements.—The spectra were recorded at the Laboratoire d'Utilisation du Rayonnement Electromagnétique (LURE) with the EXAFS III and with the dispersive-mode EXAFS spectrometers. The synchotron radiation was produced by a storage ring operated with 1.85 GeV positions and an average intensity of *ca.* 150 mA. The EXAFS III spectrometer is equipped with a two-crystal Si 311 monochromator, using air-filled ionization chambers. Harmonic rejection was performed by slightly detuning the parallelism of the crystals. The spectrum was recorded step by step, every 0.25 eV, with 1 s accumulation time per point. The spectrum of an iron metallic foil was recorded periodically to check the energy calibration. This insured an energy accuracy of 0.25 eV. The EXAFS spectra were recorded in the same way, within a 1000 eV energy range, with 2 eV steps.

The dispersive-mode EXAFS spectrometer has been described elsewhere.[17b,21] It combines focusing dispersive X-ray optics and a position-sensitive detector. The dispersive X-ray Bragg reflector consists of a 23 cm long, 1 mm thick, triangle-shaped, bent Si 311 crystal. The crystal has been asymmetrically cut (−12°) to improve the energy resolution. A down-stream mirror included in the beam path insured harmonics rejection. The sample was located at the polychromatic focus point of the

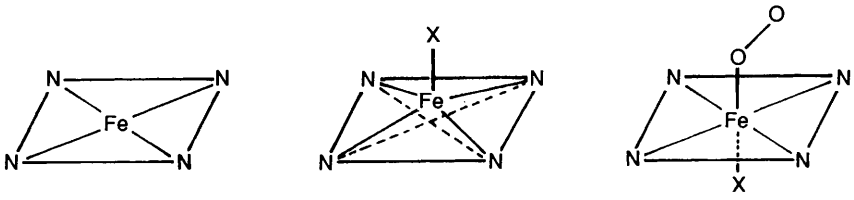

Square planar — Square pyramidal — Octahedral

D_{4h}, Fe^{II}, $S = 1$ — C_{4v} { Fe^{III}; X = Cl, OH, or O; $S = \frac{5}{2}$ / Fe^{II}; X = N(imidazole); $S = 2$ } — C_{4v}, X = N (imidazole) diamagnetic

Table 1 Intensity* and energy (eV) of the main absorption bands of the iron porphyrin complexes

	Pre-edge		Ramp		Edge		Post-edge	
Compound	P_1	P_2	B_1	B_2	C_1	D_1	D_2	C_2
1	7108.0w	—	7112.6s	7120.0w	7124m	7132s	7135vw	7139w
3	7108.2w	7111.1vw	—	7118w	7123.5s	7134m	—	7142w
4	7108.8m	7111.6vw	7116vw	7120m	7126.4s	7133m	—	7142w
5	7108.6m	7112.0vw	—	7119.4m	7125m	7133s	—	7142w
6	7109.4m	—	7115vw	7121m	7127.4s	7134m	—	7143w

m = Medium, s = strong, v = very and w = weak.

X-ray beam whereas the detector position was set at the monochromatic focus point to achieve a resolution of 1 eV. The acquisition time was typically 250 ms × 8 for the solid samples and 18s × 8 for the toluene solutions, in order to obtain each spectrum from roughly 10^{10} photons s^{-1}. As in the scanning-mode experiment, an iron metallic standard was regularly used to calibrate the energy scale of the linear detector. For the kinetic measurements the acquisition time was 10 or 20 s per spectrum, without delay between two spectra.

Data Processing.—XANES. All the spectra were treated as follows. From the experimental spectrum was subtracted a linear background, determined by least-squares fitting of the pre-edge set of experimental points. We used as energy reference the first maximum of the first derivative of the metallic foil spectrum, corresponding to the first inflection point in the absorption curve; the value retained for this point was 7111.2 eV. This value works as well as the zero of the energy scale for the dispersive data. The spectra were normalized by taking the atomic absorption as the unit of absorbance. The energies of pre-edge transitions were determined by fitting the experimental curves with polynomial functions and by taking the first and the second derivatives. Data processing was carried out using our programs on microcomputers.

EXAFS. The EXAFS analysis followed a classical method, already described.[22] After the subtraction of the background and of the atomic absorption μ_0, we obtained the $\chi(k)$ EXAFS signal in k-space, which was Fourier transformed in real space using a factor k^3. We then filtered the region of interest in the Fourier transform, using a Hamming window, and performed an inverse Fourier transform back to the k-space. The first two shells were analysed by a two-shell least-squares fitting procedure with the help of the MINUIT program[23] and tabulated amplitudes and phase shifts from Teo and Lee.[24] We checked that these tabulated values work correctly for several standards provided an adjustment of E° which allows a definition of the wave-vector, with $k = [2m/\hbar(E - E_0)]^{\frac{1}{2}}$. Therefore, E° was included as a fitting parameter for the two shells. Its value was kept in the range 7130 ± 4 eV. This value, well above 7111.2 eV, shows that the Teo and Lee phase shifts using the $Z + 1$ approximation for the fully relaxed potential is an overestimation for the Coulomb core–hole interaction. The mean free path of the photoelectron was considered as linear in k, the proportionality constant being a fitting parameter. The number of neighbours was fixed (four equatorial nitrogen atoms and one axial neighbour) and a scaling factor was introduced as a fitting parameter. Its value was close to 1 (1.2 for the hydroxo compound **4** and 1.03 for the chloro compound **5**). The Fe–C_α and Fe–C_{meso} distances were simply obtained by using the Beni and Lee[25] criterion with a phase correction for the iron–carbon pair. The whole procedure used programs written by Michalowicz.

Results

XANES.—Dioxygeniron(II) *and hydroxoiron*(III) *derivatives.* The experimental data are shown in Fig. 1 in the form of absorbance *vs.* energy for compounds **1**(*a*), **3**(*e*) and **4**(*d*). The values of the energies and a qualitative estimation of the absorbances are shown in Table 1. The spectra show common absorption bands and features labelled P_1, B_1, B_2, C_1, D and C_2. Our labels are similar to the ones of Bianconi *et al.*[15a] for the polarized spectrum of carbonyl myoglobin, Smith *et al.*[15b] for the square-planar $[CuCl_4]^{2-}$ complexes, and Kosugi *et al.*[15c] for $[Ni(CN)_4]^{2-}$.

The spectrum of compound **1** [Fig. 1(*a*)] includes a weak and badly defined pre-edge transition, P_1 (2.3% of the maximum absorbance), a well resolved peak B_1 in the edge ramp, followed by a loosely defined shoulder B_2, two main edge transitions, C_1 and D, a shoulder C_2 following the main edge, and the first EXAFS oscillations E_1 and E_2 at higher energy. The full spectrum closely resembles those already reported for porphyrins.[13d] With the chosen reference energy, P_1 peaks at 7108.0 eV.* The most striking feature of the spectrum is the well resolved peak B_1 at 7112.6 eV, 4.6 eV above peak P_1, with a strong intensity (38% of the maximum absorbance), as is generally found for square planar or linear configurations.[26]

* This value is in agreement with other values found for iron(II) complexes. Nevertheless, it is difficult to compare absolute energies from different published data since there is no general agreement on the standard reference values. We therefore focus in the discussion mainly on the shifts rather than on the absolute values.

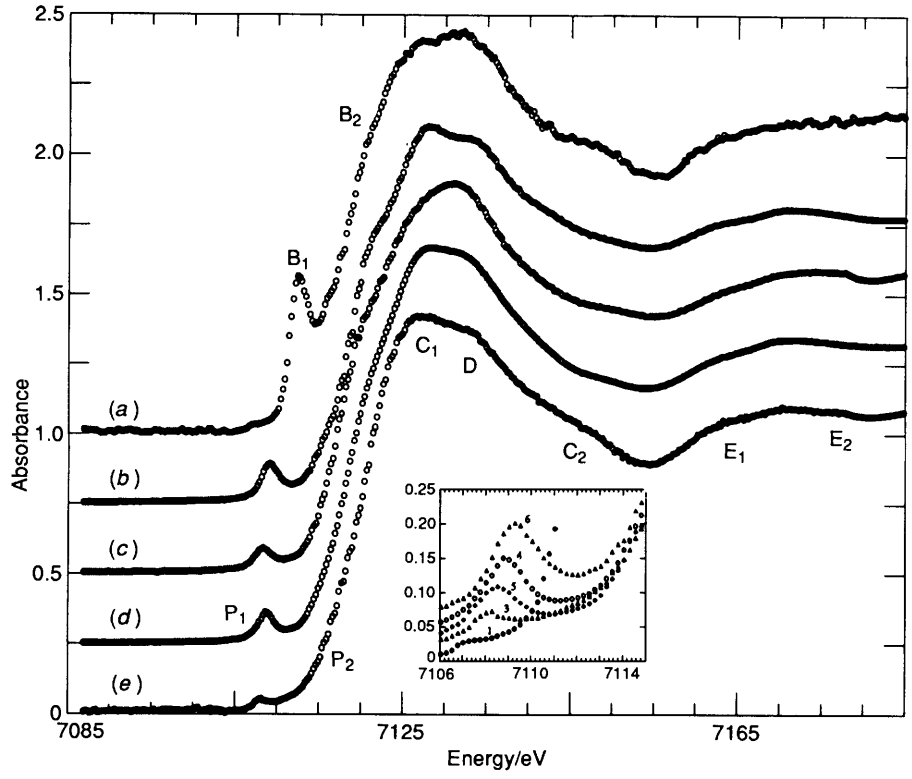

Fig. 1 Iron K-edge spectra of (*a*) square-planar compound **1** (0.01 mol dm^{-3} toluene solution), (*b*) square-pyramidal **6** (solid), (*c*) square-pyramidal **5** (solid), (*d*) square-pyramidal **4** (solid) and (*e*) octahedral **3** (solid). Insert: expanded-scale view of the pre-edge region

Table 2 Main distances (Å) around the iron in porphyrin complexes (X-ray diffraction)

Compound	7[a]	8[b]	5[c]	6[d]
Fe–N_{por}	1.979	2.072	2.060	2.087
Fe–X	2.068	2.095	2.207	1.763
Fe–Y	1.745	—	—	—
Δ(N_4 plane)	0.0	0.40	0.46	0.50
Δ(core)	0.0	0.43	0.45	0.54

[a] [FeL′(1-mim)(O_2)] **7**: octahedral, low spin,[27] L′ = 5,10,15,20-tetra(*o*-pivalamidophenyl)porphyrinate, X = N, Y = O. [b] [FeL′(2-mim)] **8**: square pyramidal, high spin,[28] X = N(imidazole). [c] Square pyramidal, high spin,[19] X = Cl. [d] Square pyramidal, high spin,[20] X = O.

The spectrum of the oxygen adduct **3** is markedly different from that of **1**: peak B_1 is no longer observed but a weak shoulder is detected in the edge ramp. This is frequently the case for octahedral complexes, with or without axial distortion. The intensity of peak C_1 is larger than that of D. The other differences are less pronounced: the intensity of the pre-edge is larger than for compound **1** (3.8%), but remains weak as in complexes with an inversion centre (compound **3** has a $FeN_4N'O$ co-ordination sphere, point group C_{4v}, close to D_{4h}). The main point to retain is the 7108.2 eV energy of the P_1 pre-edge of compound **3**, weakly shifted with respect to P_1 in compound **1** (+0.2 eV).

The P_1 pre-edge of compound **4** is more intense (7.8%), as it is generally found in iron(III) complexes without an inversion centre. The enhanced intensity is the first sign of FeN_4OH square-pyramidal surroundings. The energy of the P_1 peak is shifted towards higher energy, at 7108.8 eV. This is the usual trend when a metallic centre increases its formal oxidation state. Another striking feature is the well marked shoulder in the rising edge. The top of the edge still comes from the two transitions C_1 and D, but it is narrower than for the two previous compounds. The C_2 peak has almost disappeared, and the E_1 and E_2 EXAFS oscillations are well resolved.

Square-pyramidal iron(III) *compounds* **5** *and* **6**. Fig. 1 shows the spectra of compounds **5** (*c*) and **6** (*b*). The intensity and energy values of the bands are in Table 1, whereas Table 2 gives the geometrical data for both compounds, from X-ray diffraction (XRD).

We recorded the spectrum of the chloroiron(III) analogue of compound **5** with R = $(CH_2)_{12}$. It is not shown since it is practically identical to that of compound **5**: the nature and the length of the handle-type chain, when sufficiently long, do not modify the main features of the spectrum: smooth pre-edge of medium intensity, shoulder in the edge ramp, peak D more intense than C_1, well resolved bands E_1 and E_2. The energy of the pre-edge absorption of **5** is 7108.6 eV, at slightly lower energy than that of compound **4** but higher than that of **1**.

As for compound **6**, its spectrum presents the most intense pre-edge of the whole series (8.9%) at 7109.4 eV, a prominent shoulder at 7121 eV, and a peak C_1 at 7127.4 eV, more intense than peak D.

Square-pyramidal iron(II) *complex* **2**. The XANES spectrum of the square-pyramidal iron(II) compound **2**, recorded in the dispersive mode, is in Fig. 2. It is a dilute-solution spectrum ($\approx 5 \times 10^{-3}$ mol dm^{-3}) since we could not handle safely the compound in the solid state since it reacts readily with dioxygen to give the oxygen adduct **3**. As in the spectrum of compound **1**, the pre-edge region is not well defined. The spectrum presents a well defined shoulder in the edge ramp; peaks C_1 and D are not resolved, but C_1 is slightly higher than peak D.

EXAFS.—We aimed to measure the Fe–O distance in compound **4**. For the sake of consistency the EXAFS of this compound and of the related model **5**, the XRD structure of which was elucidated,[19] has been measured. The EXAFS signals are presented in Fig. 3, the Fourier transform in Fig. 4, and the inverse transform of the first two filtered shells and the best computed fit in Fig. 5. The results of the fits for the first Fe–N and Fe–Cl or Fe–OH, and the estimation of the different Fe–C distances, are given in Table 3.

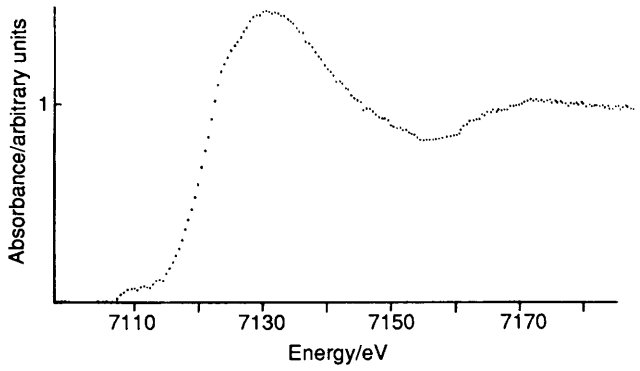

Fig. 2 Near-edge spectrum of compound **2**, recorded in the dispersive EXAFS mode (5×10^{-3} mol dm^{-3} toluene solution)

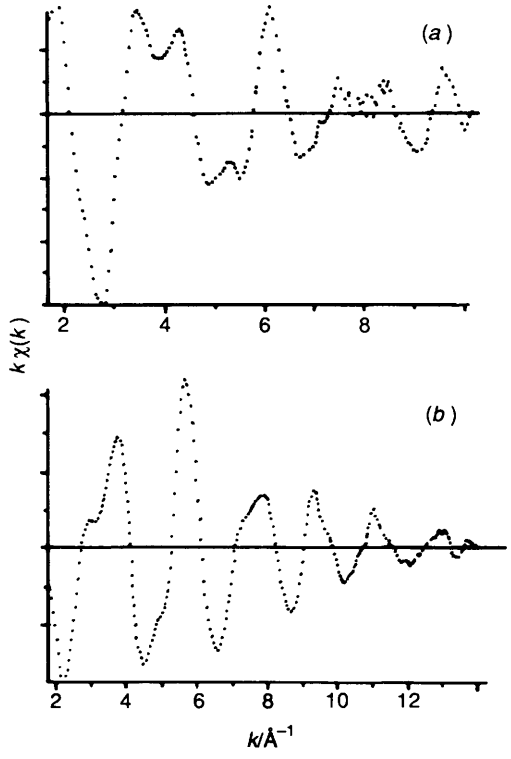

Fig. 3 Plots of EXAFS $k\chi(k)$ signal *vs.* the wave vector k for the square-pyramidal complexes **4** (*a*) and **5** (*b*)

Table 3 EXAFS data for iron basket-handle porphyrins: main distances (Å) around the iron

Compound	Bond	Distance/Å XRD	Distance/Å EXAFS	Debye–Waller $2\sigma^2/Å^2$	ρ(%)
5	Fe–N	2.06	2.06	0.0032	1.5
	Fe–Cl	2.21	2.24	0.008	
	Fe–C_α	3.09	3.09		
	Fe–C_{meso}	3.48	3.49		
4	Fe–N		2.08	0.005	3.4
	Fe–O		1.94	0.0018	
	Fe–C_α		3.10		
	Fe–C_{meso}		3.49		

The Fourier transforms in Fig. 4 exhibit peaks characteristic of porphyrins: peak 1 comprises the in-plane Fe–N_{por} and the axial Fe–X distances which are not resolved. Peaks 2 and 3 can be assigned to the eight C_α and the four C_{meso} atoms, whereas peak 4 is clearly due to the eight C_β carbons of the macrocycle. The most striking difference in the two spectra is related to the

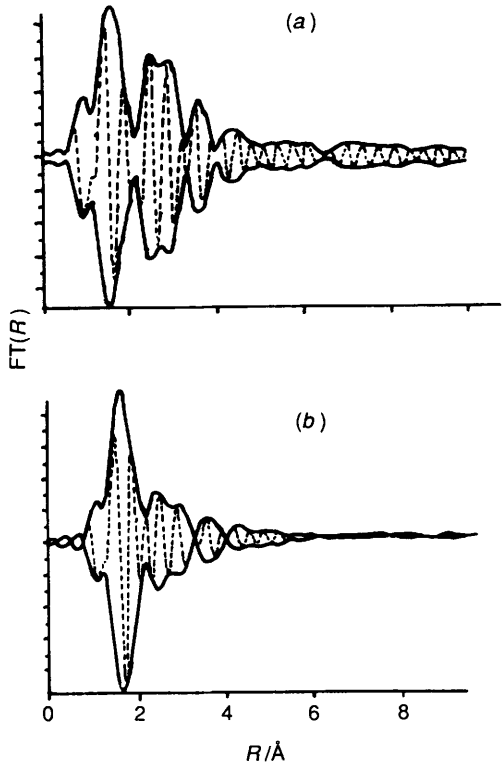

Fig. 4 Fourier transforms FT(R) in real space of the $k^3\chi(k)$ EXAFS signal for compounds **4** (*a*) and **5** (*b*)

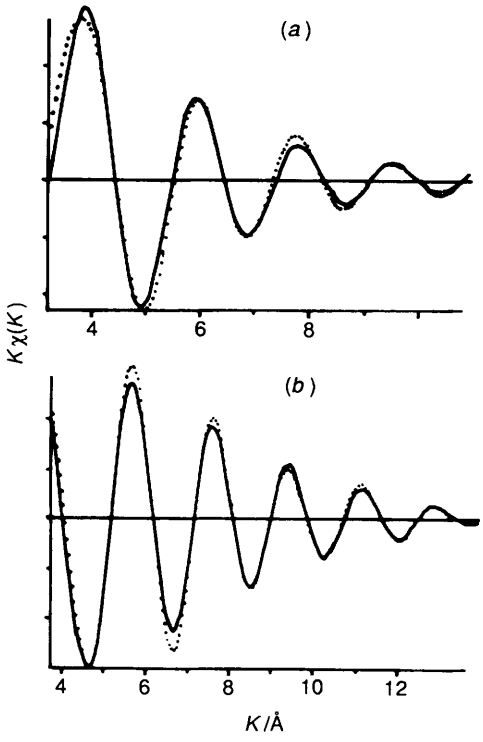

Fig. 5 Inverse Fourier transform in k space of the filtered R-space first shell for compounds **4** (*a*) and **5** (*b*). Experimental (full line) and best theoretical two-shell fit (dotted line)

relative amplitude of the first and of the other peaks: the first peak appears more intense in the spectrum of the chloro compound [Fig. 4(*b*)].

Turning now to the quantitative data analysis (Table 3), we point out the close correspondence between the XRD results and those obtained by EXAFS. This shows that the method of extraction of the unknown Fe–N_{por} and Fe–OH distances in the

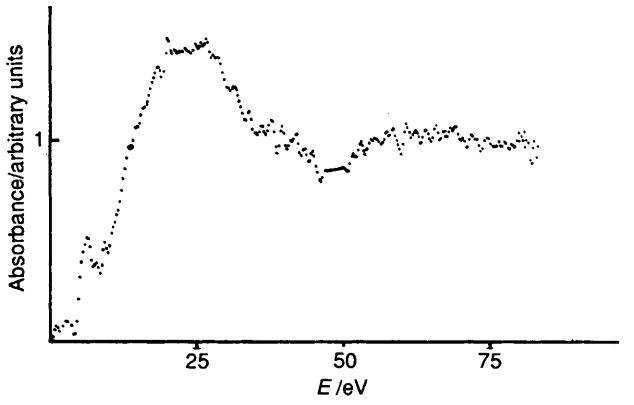

Fig. 6 Spectrum recorded in the dispersive mode during the kinetic oxidation of compound **1**, after data processing: t = 20 s, 0.4 eV per data point resolution (averaging over 4 pixels) and accumulation time (40 s)

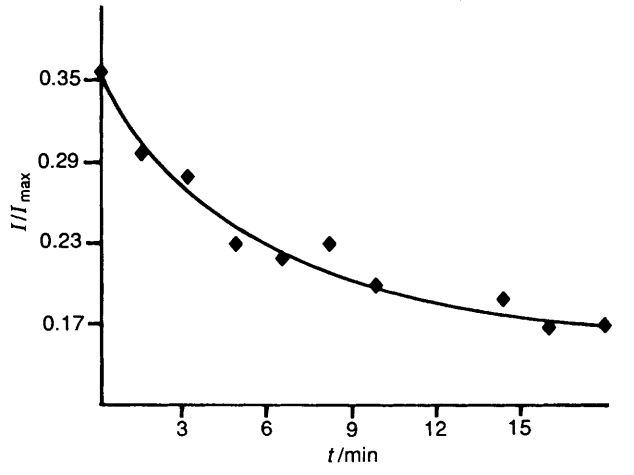

Fig. 7 Evolution of the relative intensity of the B_1 7112.6 eV feature of compound **1** *vs.* time at room temperature, 0.01 mol dm^{-3} toluene solution saturated with dioxygen

Table 4 The Fe–O axial distances determined for different porphyrins by X-ray diffraction or EXAFS experiments

Compound	Fe–O/Å	Ref.
$[Fe(tpp)(H_2O)_2]$	2.095	27
$[Fe(tpp)(OClO_3)]$	2.029	28
$[\{Fe(tpp)\}_2O]$	1.763	20*b*
[FeL'(1-mim)(O_2)]	1.75	14*j*,29
[FeL'(2-mim)(O_2)]	1.90	14*j*,30

hydroxo compound can be considered as reliable. We found four nitrogen atoms at 2.08 Å and one oxygen atom at 1.94 Å with a two-shell fit merit factor of 3.4%.

Kinetics.—The spectra of the square-planar iron(II) **1** and of the hydroxoiron(III) species **4** [Fig. 1(*a*), (*d*)] are sufficiently different to use XANES as a local structural probe of the absorbing centre to follow the kinetics of oxidation, provided the reaction time ranges between a few tens of seconds and a few tens of minutes. We performed such kinetic measurements *in situ*, at room temperature, *i.e.* 20 °C. The molarity of the porphyrin solution was about 10^{-2} mol dm^{-3}. The porphyrin used was compound **1**.

At time t = 0 we introduced dioxygen gas into the toluene solution, using the automatic electromagnetic valve and the magnetic stirrer. In this way the solution is saturated with an excess of dioxygen within a few seconds. For the first 60 spectra the accumulation time was 10 s, without delay between each spectrum. The following spectra were accumulated during 20 s, without delay between each spectrum. Between the two series of measurements, the data were transferred to the computer hard-disk.

In the experimental spectrum the interval between two pixels is roughly 0.1 eV. A glitch appears above pixel 600, due to an extra Bragg reflection for this specific dispersive crystal orientation. The signal/noise ratio is low: at the edge, the jump represents 1% of the total absorbance signal, due to the toluene solution. To improve the quality of the signal in order to reach quantitative conclusions we added four spectra (total accumulation time 40 s); a linear background was subtracted by fitting the pre-edge part. Then, for each spectrum, we performed a mean through four consecutive points: in other words we reduced the temporal resolution to 40 s and the energy resolution to 0.4 eV which is smaller than the overall resolution $\approx$1 eV. This treatment significantly improved the signal/noise ratio as shown in Fig. 6. We were then able to follow the relative intensity I/I_{max} of the B_1 absorption band at 7112.6 eV with time (Fig. 7). The half-life of the oxidation reaction, $t_{\frac{1}{2}} \approx 6$ min.

Discussion

Our discussion will focus on three points: (1) the Fe–O distance in compound **4**, as determined by EXAFS; (2) the changes in the XANES spectra related to the stereochemistry, to the oxidation and to the spin states of the iron ion; (3) the significance of the kinetic result.

EXAFS.—The close correspondence between the XRD and EXAFS results for the model compound **6** allows us to be confident in the EXAFS value of the Fe–O distance in the hydroxy compound **4**. The computation is not an easy task,[13,14*f*,*k*] and the shorter the Fe–O distance the more difficult is the determination[14*k*] due to interference by the Fe–N distances. One problem is the correlation between the fitting parameters. Such correlations appear more marked for the amplitude parameters (Debye–Waller factor, mean free-electron path) than for the phase parameters. Furthermore, the fit reported in Table 3 was the only one corresponding to reasonable values of the agreement factor and of the fitted parameters. When we did not take into account a short Fe–O axial distance, a poor agreement factor and unreliable $Fe–N_{por}$ distances were output. The uncertainty in the distance determination can be evaluated as $\pm$0.02 Å for $Fe–N_{por}$ and $\pm$ 0.03 Å for Fe–O.

To the best of our knowledge, our result is the first Fe^{III}–OH distance obtained from EXAFS measurements on an iron porphyrin. Previously, only $Fe–O_2$[14*j*] or Fe=O[14*f*,*h*] distances were determined in similar tetrapyrrolic derivatives. The axial Fe–O distances of some porphyrins are reported in Table 4.

The proposed distance in compound **4**, Fe–O 1.94 $\pm$0.03 Å, is very close to the only Fe^{III}–OH distance previously determined by XRD in a distorted porphinoid macrocycle (1.89 Å). It is shorter than the distance found in $[Fe(tpp)(H_2O)_2]^+$ and in $[Fe(tpp)(OClO_3)]$. It is much larger than the Fe–O distance in Fe^{IV}–O horseradish peroxidase or in low-spin [Fe^{II}(PF)(1-mim)(O_2)] [Fe–N(imidazole) 2.068 Å] but close to that in [Fe^{II}L'(2-mim)(O_2)] [Fe–N(imidazole) 2.107 Å]. One can infer from the present value of the Fe–O distance that the Fe^{III}–OH bond is obtained by the oxidation of the square-planar iron(II) complex. The similarity of our EXAFS-derived $Fe–N_{por}$ distance, 2.08 Å $\pm$ 0.02 Å, with the ones determined by XRD in square-pyramidal Fe^{III} porphyrins which range from 2.06 to 2.09 Å[31*a*] confirms this conclusion. Assuming a porphyrinic hole of 4.05 Å, this allows to determine that Fe sits out of the plane of the four pyrrolic nitrogen atoms by about 0.47 Å. To go further in the analysis of this particularly controversial point, in particular to obtain this distance directly from the data, through the use of the strong multiple scattering effects present in porphyrins, it would be necessary to use more

sophisticated EXAFS treatments, such as the difference Fourier transform[13a] or restrained refinement approach[14l] which have been applied with success to porphyrins and proteins. This is beyond the scope of the present paper.

XANES.—Pre-edge. (*i*) Our data verify the influence of symmetry on the intensity of the pre-edge P_1. In the square-planar D_{4h} complex **1** the intensity is low; it increases from the distorted octahedron $FeN_4N'O$ **3**, to the square-pyramidal FeN_4X, with X = O in **6**, where the distance *d* of the iron ion out of the porphyrin N_4 plane is maximum, at 0.5 Å (Table 2). This band is now firmly established as a transition of the photoelectron from the 1s level to an excited state implying the molecular orbitals (MOs) corresponding to d orbitals.[14,15] Roe *et al.*[32] have already shown how the increase in intensity of the pre-edge may be related to the increased mixing of the 4p(Fe) orbital in the molecular orbitals containing the 3d(Fe): in the sequence $O_h \longrightarrow C_{4v} \longrightarrow T_d$, the larger the mixing, the more intense is the transition.

(*ii*) As for the oxidation state of the oxygen adduct **3**, the energy of P_1 is close to the value exhibited by the iron(II) compound **2**. Unfortunately, the iron(II) spectrum in solution is of poor quality. Nevertheless, the calculated mean value, 7108.0 eV, is close to that obtained with the oxygen adduct **3**, at 7108.2 eV. On the other hand, the P_1 peak of iron(III) porphyrins [Fe(por)X] has at higher energy: $E(X = Cl)$ in **5** < $E(OH^-)$ in **4** < $E(O^{2-})$ in **6** and d(Fe–X) = 2.20,[19] 1.94, 1.76 Å.[31b] As already stated by Eisenberger *et al.*,[14a] this behaviour can be interpreted by two simultaneous effects: (*a*) a ligand-field effect, the shorter the distance and the larger the Fe–X overlap, the more destabilized are the d MOs; since the d MO are non-bonding or weakly antibonding, this effect is small; (*b*) a charge-transfer effect, the more ionic the Fe–X bond the larger is the real atomic positive charge on the Fe, the lower is the energy gain due to the electron relaxation, and the higher is the final state. These effects are weak but observable (experimental uncertainty on the energy ≈ ±0.3 eV).

The shift of the pre-edge to higher energy is not observed in the oxygen adduct **3**, which can be formulated better as $Fe^{II}(O_2)$ than $Fe^{III}(O_2^-)$. An analogous study with the dioxygen adduct of haemoglobin, came to the opposite conclusion.[14b,h]

(*iii*) The spin state of the complexes changes from $S = 0$ (diamagnetic) in the oxygen adduct **3**, to $S = 1$ in the square-planar **1** and to $S = \frac{5}{2}$ in the different square-pyramidal complexes **4**–**6**. It does not appear to be of prime importance in these K-edge spectra, in contrast to what happens in less-constrained complexes[33] or at the L_{III}, L_{II} edges, which are for obvious symmetry reasons much more sensitive probes of the d states than is the K edge.[34]

(*iv*) Another striking point is the width of the P_1 peak in the spectra of the three iron(III) porphyrins in [Fig. 1(*b*)–(*d*)]: the width is 2.4 eV for the hydroxy derivative **4** and 2.8 eV for the chloro **5** and in the oxo **6** derivatives; this is not expected *a priori* from simple ligand-field considerations[14a,35] from which one expects an increase in the band width in the order $Cl^- < OH^- < O^{2-}$. The band narrowing with **4** appears specific to this compound and may be related to a smaller motion of the hydroxy ligand.

Very weak transitions are present at 7111–7112 eV (P_2) for compounds **3**–**5** and at 7115 and 7116 eV (B_2) for **6** and **4** (Table 1). In the present state of the art one may invoke two-electron transitions, but the theory has not been established to put this assignment on a firmer ground. We observed systematically such P_2 transitions in complexes with ligands having π and π* orbitals.[33,36,37]

Rising edge. We comment now on the characteristics of peak B_1 in the spectrum of compound **1** and of the shoulders observed in the edge of square-pyramidal complexes **4**–**6**. Two points are striking about peak B_1: its intensity and its energy. (*i*) The intensity is strong: the transition is allowed, and has been already shown to be *z*-polarized for similar square-planar complexes. (*ii*) The gap in energy between structures P_1 and B_1 is much smaller (4.6 eV) than the difference in atomic energy levels tabulated by Moore.[38] In the iron case, $\Delta E = E(3d^5, 4p^1) - E(3d^6, 4p^0) = 11$ eV for Fe^{II} and $\Delta E = E(3d^4,4p^1) - E(3d^5) = 24$ eV for Fe^{III}. In the all-electron *ab initio* calculations by Bair and Goddard[26] and Kosugi *et al.*[15c,d] such bands are described as (1s ⟶ $4p_z$ + shake-down) transitions. Within this framework, a formal L⟶M charge transfer occurs in the final state, associated with a $4p_z$ transition. The energy of the band is lower than that of the 'pure' 1s ⟶ $4p_z$ transition and depends on the electronegativity of the ligand L, on the initial d atomic orbital energy and occupancy and on the magnitude of the core–hole attractive potential (electrostatic interaction, Coulomb and exchange interactions). A totally equivalent description takes into account the relaxation of the metallic orbitals of the absorber due to the Coulomb interaction created by the core hole (when the orbitals of the ligand remain practically unperturbed) and describes the transition as 1s ⟶ $4p_z$ in a fully relaxed configuration ($1s^1 \cdots 3d^{n+1}\ L^1 4p_z^1$). At higher energies, a weaker two-electron transition can occur ($1s^1 \cdots 3d^n\ L^2 4p_z^1$). We observed in square-planar metalloporphyrins of different divalent metal ions a trend in the energy of the B_1 band, from 4.6 eV for Fe^{II} to 6.2 eV for Co^{II} and to >8 eV for Cu^{II}. This is consistent with the decrease in energy of the metal d orbitals implied in the relaxation process with increasing atomic number *Z*. We are currently checking this trend in bivalent metalloporphyrins. The small energy gap between the P_1 and B_1 peaks confirms the nature of the transition of the core electron to a fully relaxed excited state.

The increase in energy of the B_2 shoulder in spectra of compounds **5** (7119.4, $X = Cl^-$), **4** (7120, $X = OH^-$) and **6** (7121 eV, $X = O^{2-}$) is weak but may be related to a larger destabilization of the $4p_z$ orbital (oxidation state and ligand-field effect), combined with a charge-transfer energy stabilization larger in the chloro than in the μ-oxo derivative. Such an increase in energy with shortened axial distances and increased electronegativity of the axial ligand is also observed in square-planar complexes with an equatorial ligand L.[39] This is also the case for the energy of the shoulder in square-pyramidal complexes when the M–X distances and electronegativities of the axial ligand X are varied, for example in cobalt(III) porphyrins with X = F, Cl or Br[36] or in iron(III) phthalocyanines.[37]

To conclude the edge-ramp discussion, we would stress the clear demonstration provided by our data that the so-called 'edge energy' (*i.e.* the energy of the first inflection point in the edge) can, by no means, be considered as representative of the oxidation state of a compound. This energy, for a given oxidation state, is largely dependent on the stereochemistry of the complex: the existence of transitions like B_1 in D_{4h} square-planar entities or shoulders like B_2 in C_{4v} square-pyramidal compounds precludes a reliable correlation between the inflection point energy and the oxidation state. Consequently, the inflection point (which has by itself no physical meaning in insulating materials) must be used very carefully in the characterization of an oxidation state.

Edge top. We comment now on the evolution of the two bands at the top of the edge. Table 1 gives qualitatively the intensity of the absorption bands. To the best of our knowledge, peaks C_1 and D are present, with different relative intensities, in the spectra of all porphyrin analogues. Experimental polarization studies of carbonyl myoglobin[15a] and highly oxidized porphyrins[15e] substantiated by multiple-scattering calculations concluded that peak C_1 is essentially *z*-polarized, whereas peak D corresponds mainly to *x*,*y*-polarized transitions, corresponding to structural events within the plane of the macrocycle. The presence of new axial ligands gives rise to new multiple-scattering *z*-polarized resonances with changes in the C_2 transition.

The transitions are allowed and are generally attributed to 1s ⟶ 4p MO transitions, either *z*- or *x*,*y*-polarized. The *x*,*y*-

polarized transitions lie at higher energy given the larger destabilization of the 4p (x,y) orbitals by the tetrapyrrolic nitrogen atoms. Polarization experiments on elongated tetragonal complexes with two axial ligands at various distances have shown that the z-polarized transition (C_1) changes mainly in intensity and is roughly constant in energy.[15b]

In our case it is clear from the spectra that the relative intensity of the two peaks C_1 and D is closely dependent on the nature of the axial subsituent X. When no ligand X is present (compound **1**) or when the axial substituent is heavy or/and at a long distance (compound **5**) peak C_1 is weak or may even appear as a simple shoulder. On the contrary, light X ligands [N(from imidazole), OH, O], of increasing electronegativity and closer to the iron, give rise to an enhancement of the intensity of the C_1 peak. Such an influence of the nature of X (F, Cl, Br or I) and of the distance M–X is also verified in other series of axially substituted tetrapyrollic macrocycles.[36,37] This phenomenon may be related to (*i*) the real charge borne by the metal, the more electronegative the ligand X, the more ionic the bonding, the more available are the vacant p orbitals (such an enhancement of the 'white line' with the oxidation state of heavy metal compounds has often been put forward[40] at the L edge); (*ii*) the back scattering amplitude of the axial ligands, in a multiple-scattering approach. The two interpretations are different ways of looking at the phenomenon and, in our examples, of foreseeing the same evolution of the spectra. Indeed, the XANES features, close to the edge, deal with atomic-like transitions and cluster-like transitions as well. In the last case, the probed partial density of the state can be simulated either by a molecular orbital (or band structure) calculation or by a multiple scattering approach.

In the case of a simple cluster structure, a molecular orbital (or a band structure) calculation (accounting for the relaxation in the final state) should be better able to give a significant picture of the environment investigated. As for the energies of the two transitions C_1 and D, there is no large shift to higher energy when going from oxidation state II to III, contrary to the phenomenon observed in haemoproteins.[14b,h] The energy of peak D is at 7133.5 ± 0.5 eV for all the compounds, except **1**. This behaviour is consistent with the rough constancy of the $Fe–N_{por}$ distances in compounds **4**–**6**, which have the same oxidation state. This is correlated to the variation of the oxidation state for compound **1**: there is a +2 eV shift of D from compound **1** (Fe^{II}, intermediate spin) to **6** (Fe^{III}, high spin). Finally, the contraction of the in-plane distances in the diamagnetic dioxygen adduct, **3** (found at 1.98 Å by XRD in the analogue described in Table 2) compared to the 2.08 Å in [{Fe^{III}(tpp)}$_2$O] **6** (Table 2) appears to counterbalance the influence of the oxidation state since the energy of D is the same for compounds **3** and **6**.

The evolution of the energy of the C_1 peak is more important and perhaps clearer, since the axial events are larger: the peak shifts from 7123.5 eV in compound **3** (oxygen adduct) to 7127.4 eV in **6**. The values for the iron(II) compounds are at practically the same energy (7123.7 ± 0.3 eV) and the iron(III) compounds exhibit higher energy and show a shift towards higher energy from the chloro compared to the μ-oxo compound, in the direction expected from a contraction of the Fe–X distances and/or a more ionic iron.

We would like nevertheless to conclude this part of the discussion with a warning on the possibility of reaching definitive conclusions on the nature of the absorption bands in the edge using only isotropic powder results. Polarization-dependent spectral experiments with orientated single crystals are necessary to insure correct assignments. Studies of series of compounds such as the one presented herein are useful to isolate the influences of some parameters, when their effects are not too intricate, and to test hypotheses, but by no way can one derive definite answers when only powder or solution data are available.

Kinetics.—The present kinetic study has to be considered as a very preliminary one. Even if the dispersive EXAFS station allows recording of spectra of very dilute solutions when prolonged data accumulation is possible, the problem at hand in kinetics is a trade off between the time resolution and the signal/noise ratio: we have already stated that it is necessary to extract structural information from changes in a signal which by itself represents only 1% of the total absorbance, dominated by the solvent. Furthermore, the solubility of the oxidation products is lower than that of the initial reagent and a precipitate can occur which significantly limits the observation time. Other experiments are planned, particularly with hanging base derivatives.

From the existing experimental results[41] the reaction scheme in equations (2)–(6) may be proposed (H_2L = basket-handle

$$[FeL] + O_2 \underset{k_{-1}}{\overset{k_1}{\rightleftharpoons}} [FeL]\cdot O_2 \quad (2)$$

$$[FeL]\cdot O_2 + H_2O \xrightarrow{k_2} [FeL \cdots O_2^{\cdot -} \cdots HOH] \quad (3)$$

$$[FeL \cdots O_2^{\cdot -} \cdots HOH] \longrightarrow [FeL(OH)] + HO_2^{\cdot} \quad (4)$$

$$2\,HO_2^{\cdot} \longrightarrow H_2O_2 + O_2 \quad (5)$$

$$H_2O_2 \longrightarrow H_2O + \tfrac{1}{2}O_2 \quad (6)$$

porphyrin). Water is always present in small amounts in the toluene solution as can be seen from the preparation procedure. The formation of H_2O_2 has recently been demonstrated by measurements with [^{17}O]dioxygen, which led to $H_2{}^{17}O_2$.[41] The constants k_1 and k_{-1} have been measured ($-\log k_1 = 8$ and $\log k_{-1} = 4$)[1d,2] which shows that the dioxygen adduct is not a stable species. From the above scheme the simple kinetic

$$v = -d[FeL]/dt = k_1[FeL][O_2](1 - k_{-1})/(k_{-1} + k_2[H_2O]) \quad (7)$$

law (7) can be derived. In presence of an excess of dioxygen, as in our experiment, the kinetics is expected to be first order in [L] if $k_{-1}/(k_{-1} + k_2[H_2O]) \ll 1$ or $k_2[H_2O] \gg k_{-1}$.

Our X-ray absorption spectral results, alone, are unable to lead to the formulation of such a mechanism. Nevertheless, our observations are consistent with the above scheme. (*i*) The dioxygen adduct is not observable with compound **1** as the starting reagent; we studied the kinetics by following the intensity of the peak B_1, which disappears progressively, demonstrating that the dioxygen adduct is not produced in detectable amounts when saturating the toluene solution with dioxygen. This is in line with the values of k_1 and k_{-1}. The situation is different with compound **2**. In this case the dioxygen adduct is stable and can be detected by X-ray absorption just after the switching of the electromagnetic valve and the introduction of dioxygen. The formation of this dioxygen adduct is too rapid to be followed at the present state of development of our technique. (*ii*) The product of the reaction is the hydroxy species **4**. (*iii*) We can use the evolution of the absorbance at 7112.6 eV, at time t, $A(t)$, from its value at time $t = 0$, $A(0)$, to its value at infinite time, $A(\infty)$, to construct a plot $\log\{[A(0) - A(\infty)]/[A(t) - A(\infty)]\}$ *versus* time, which is expected to be linear for first-order kinetics. Within the uncertainty of our data, the plot is linear at the beginning of the kinetics giving an apparent initial rate constant $k' = k_1[O_2]$ which can be approximated as 9 min^{-1} (hence a half-life equal to about 6 min). Then, the line curves downwards as expected if the $k_2[H_2O]$ term in equation (7) decreases.

Conclusion

We have presented in this work X-ray absorption spectral data for a series of synthetic basket-handle porphyrins, in various oxidation and spin states. Our results show that in such synthetic haemoprotein analogues the dioxygen adduct **3** may be better formulated as $Fe^{II}(O_2)$ than by $Fe^{III}(O_2^-)$, which was proposed for the biological oxyhaemoglobin and oxymyoglobin analogues. We have given the first structural characterization of a hydroxoiron(III) basket-handle porphyrin derivative and proposed a Fe–O bond length of 1.94 ± 0.03 Å in this compound. The first (preliminary) kinetic data for the oxidation of an iron(II) to hydroxoiron(III) basket-handle porphyrins are presented. We intend to pursue these studies better to analyse and characterize oxygenated states and the oxidation kinetics of such synthetic analogues of haemoproteins.

References

1 (*a*) J. P. Collman, R. R. Gagne, C. A. Reed, T. R. Halbert, G. Lang and W. T. Robinson, *J. Am. Chem. Soc.*, 1975, **97**, 1427; (*b*) T. G. Traylor, M. J. Mitchell, S. Tsuchyia, D. H. Campbell, D. V. Stynes and N. Koga, *J. Am. Chem. Soc.*, 1981, **103**, 5234; (*c*) K. S. Suslick and T. J. Reinert, *J. Chem. Educ.*, 1985, **62**, 974; (*d*) M. Momenteau, *Pure Appl. Chem.*, 1986, **58** 1493; (*e*) W. R. Scheidt and Y. J. Lee, *Struct. Bonding (Berlin)*, 1987, **64**, 1; (*f*) B. Morgan and D. Dolphin, *Struct. Bond (Berlin)*, 1987, **64**, 115; refs. therein.

2 (*a*) M. Momenteau, B. Loock, J. Mispelter and E. Bisagni, *Nouv. J. Chim.*, 1979, **3**, 77; (*b*) M. Momenteau and B. Loock, *J. Mol. Catal.*, 1980, **7**, 315; (*c*) M. Momenteau, J. Mispelter, B. Loock and E. Bisagni, *J. Chem. Soc., Perkin Trans. 1*, 1983, 189; (*d*) M. Momenteau, J. Mispelter, B. Loock and J. M. Lhoste, *J. Chem. Soc., Perkin Trans. 1*, 1985, 61; (*e*) M. Momenteau, J. Mispelter, B. Loock and J. M. Lhoste, *J. Chem. Soc., Perkin Trans. 1*, 1984, 221; (*f*) M. Momenteau, B. Loock, C. Tetreau, D. Lavalette, A. Croisy, C. Schaeffer, C. Huel and J. M. Lhoste, *J. Chem. Soc., Perkin Trans. 2*, 1987, 249; (*g*) M. Momenteau, B. Loock, C. Huel and J. M. Lhoste, *J. Chem. Soc., Perkin Trans. 1*, 1988, 283.

3 L. Pauling, *Nature (London)*, 1964, **203**, 182.

4 J. J. Weiss, *Nature (London)*, 1964, **202**, 83.

5 G. H. Loew, *Iron Porphyrins*, eds. A. B. P. Lever and H. B. Gray, Addison-Wesley, Reading, 1983, Part 1, p. 1; A. Dedieu, M. M. Rohmer and A. Veillard, *Adv. Quantum Chem.*, 1982, **16**, 43.

6 J. B. Wittenberg, B. A. Wittenberg, J. Peisach and W. E. Blumberg, *Proc. Natl. Acad. Sci. USA*, 1970, **67** 1846; (*b*) T. G. Spiro, *Biochim. Biophys. Acta*, 1975, **416**, 169; (*c*) G. Lang and W. Marshall, *Proc. Phys. Soc.*, 1966, **87**, 3; (*d*) K. Spartalian, G. Lang, J. P. Collman, R. R. Gagne and C. A. Reed, *J. Chem. Phys.*, 1975, **63**, 5375; (*e*) M. Cerdonio, A. Congiu-Castellano, L. Calabrese, S. Morante, B. Pispisa and S. Vitale, *Proc. Natl. Acad. Sci. USA*, 1977, **74**, 398; (*f*) M. Cerdonio, A. Congiu-Castellano, L. Calabrese, S. Morante, B. Pispisa and S. Vitale, *Proc. Natl. Acad. Sci. USA*, 1978, **75**, 4916; (*g*) L. Latos-Graszynski, R. J. Cheng, G. N. La Mar and A. L. Balch, *J. Am. Chem. Soc.*, 1982, **104**, 5992; (*h*) I. Gerothanassis and M. Momenteau, *J. Am. Chem. Soc.*, 1987, **109**, 6944.

7 A. A. E. Awady, P. C. Wilkins and R. G. Wilkins, *Inorg. Chem.*, 1985, **24**, 2053; L. Fielding, G. R. Eaton and S. S. Eaton, *Inorg. Chem.*, 1985, **24**, 2309.

8 D. Lexa, M. Momenteau, M. Saveant and F. Xu, *Inorg. Chem.*, 1985, **24**, 122.

9 J. M. Cense and R. M. Le Quan, *Tetrahedron Lett.*, 1979, 3725; M. J. Gunter, L. N. Mander and K. S. Murray, *J. Chem. Soc., Chem. Commun.*, 1981, 799.

10 *Synchrotron Radiation Research*, eds. H. Winick and S. Doniach, Plenum, New York, 1980; *Handbook on Synchrotron Radiation*, eds. D. E. Eastman and Y. Farge, North-Holland, Amsterdam, 1983, vols. 1a and 1b.

11 (*a*) *EXAFS spectroscopy, Techniques and applications*, eds. B. K. Teo and D. C. Joy, Plenum, New York, 1981; (*b*) B. K. Teo, in *EXAFS, Basic principles and data analysis*, Springer, Berlin, 1986; (*c*) S. P. Kramer and K. O. Hodgson, *Prog. Inorg. Chem.*, 1979, **25**, 1; (*d*) D. Raoux, J. Petiau, P. Bondot, G. Calas, A. Fontaine, P. Lagarde, P. Levits, G. Loupias and A. Sadoc, *Rev. Phys. Appl.*, 1980, **15**, 1079; (*e*) P. A. Lee, P. H. Citrin, P. Eisenberger and B. Kincaid, *Rev. Mod. Phys.*, 1981, **53**, 769; (*f*) *EXAFS and Near Edge Structure II*, Series in Chemical Physics 27, eds. A. Bianconi, M. Incoccia and M. Stipcich, Springer, Berlin, 1982; (*g*) *EXAFS and Near Edge Structure III*, eds. J. Penner-Hahn, B. Hedman and K. O. Hodgson, Springer, Berlin, 1984; (*h*) P. Lagarde, J. Petiau and D. Raoux (Editors), *J. Phys. (Paris)*, 1986, **47**, C8; (*i*) J. Mustre de Leon, E. A. Stern, D. E. Sayers, Y. Ma and J. J. Rehr (Editors), *Physica B*, **1989**, 158; (*j*) H. Dexpert, A. Michalowicz and M. Verdaguer (Editors), *J. Chim. Phys. (Paris)*, 1989, **86**, 7; (*k*) *Synchrotron Radiation and Biophysics*, ed. S. S. Hasnain, Series in Physics and its Applications, Ellis Horwood, New York, 1989; (*l*) *X-Ray Absorption Fine Structure*, ed. S. Hasnain, Ellis Horwood, New York, 1991; (*m*) Report on the International Workshops on Standards and Criteria in X.A.F.S., *Physica B*, 1989, **158**, 701.

12 A. Bianconi, in ref. 11(*f*), p. 118; C. R. Natoli, in ref. 11(*g*), p. 43; E. I. Solomon, *Comments Inorg. Chem.*, 1984, **3**, 225; C. R. Natoli and M. Benfatto, in ref. 11(*h*), p. 11.

13 (*a*) J. Goulon, P. Friant, C. Goulon-Ginet, A. Coutsolelos and R. Guilard, *Chem. Phys.*, 1984, **83**, 367; (*b*) R. Weiss, J. Goulon, P. Friant, J. Fischer, L. Ricard and M. Momenteau, *Nouv. J. Chim.*, 1985, **9**, 33; (*c*) J. L. Poncet, R. Guilard, P. Friant, C. Goulon-Ginet and J. Goulon, *Nouv. J. Chim.*, 1984, **8**, 583; (*d*) O. Bortolini, M. Ricci, B. Meunier, P. Friant, I. Ascone and J. Goulon, *Nouv. J. Chim.*, 1986, **10**, 39; (*e*) *Iron porphyrins*, eds. H. B. Gray and A. B. P. Lever, VCH, Weinheim, 1989, p. 3.

14 (*a*) P. Eisenberger, R. G. Schulman, G. S. Brown and S. Ogawa, *Proc. Natl. Acad. Sci. USA*, 1976, **73**, 491; (*b*) S. Pin, A. Alpert and A. Michalowicz, *FEBS Lett.*, 1982, **147**, 106; (*c*) J. E. Penner-Hahn, T. McMurry, M. Renner, L. Latos-Graszynski, K. S. Eble, I. M. Davis, A. Balch, J. T. Groves, J. H. Dawson and K. O. Hodgson, *J. Biol. Chem.*, 1983, **258**, 12761; (*d*) P. J. Durham, A. Bianconi, A. Congiu-Castellano, A. Giovanelli, S. S. Hasnain, L. Incoccia, S. Morante and J. B. Pendry, *Eur. Mol. Biol. Organization J.*, 1983, 1441; (*e*) A. Bianconi, A. Congiu-Castellano, M. Dell'Ariccia, A. Giovanelli, P. J. Durham, E. Burattini and M. Barteri, *FEBS Lett.*, 1984, **178**, 165; (*f*) B. Chance, L. Powers, Y. Ching, T. Poulos, G. R. Cschonbaum, I. Yamazaki and K. G. Paul, *Arch. Biochem. Biophys.*, 1984, **235**, 596; (*g*) S. Pin, P. Valat, R. Cortes, A. Michalowicz and A. Alpert, *Biophys. J.*, 1987, 997; (*h*) A. Bianconi, A. Congiu-Castellano, M. Dell'Ariccia, A. Giovanelli, P. J. Durham and E. Burattini, *Biochem. Biophys. Res. Commun.*, 1985, **131**, 98; (*i*) A. Bianconi, A. Congiu-Castellano, M. Dell'Ariccia, A. Giovanelli, E. Burattini, M. Castagnola and P. J. Durham, *Biochim. Biophys. Acta*, 1985, **831**, 120; (*j*) G. L. Woolery, M. A. Walters, K. S. Suslick, L. S. Powers and T. G. Spiro, *J. Am. Chem. Soc.*, 1985, **107**, 2370; (*k*) J. E. Penner-Hahn, K. S. Eble, T. J. McMurry, M. Renner, A. L. Balch, J. T. Groves, J. H. Dawson and K. O. Hodgson, *J. Am. Chem. Soc.*, 1986, **108**, 7819; (*l*) S. S. Hasnain and R. W. Strange in ref. 11(*k*), p. 104; (*m*) P. F. Lindley, R. C. Garratt and S. S. Hasnain, in ref. 11(*k*), p. 176; (*n*) J. Pant, A. Abbasi, Z. H. Zaidi, R. W. Strange, G. P. Diakun, G. R. Jones and S. S. Hasnain, in ref. 11(*l*), p. 122; (*o*) P. F. Lindley, in ref. 11(*l*), p. 115.

15 (*a*) A. Bianconi, A. Congiu-Castellano, P. J. Durham, S. S. Hasnain and S. Phillips, *Nature (London)*, 1985, **318**, 685; (*b*) T. A. Smith, J. E. Penner-Hahn, M. A. Berdin, S. Doniach and K. O. Hodgson, *J. Am. Chem. Soc.*, 1985, **107**, 5945; (*c*) N. Kosugi, T. Yokohama and H. Kuroda, *Chem. Phys.*, 1986, **104**, 449; (*d*) N. Kosugi, T. Yokohama, K. Asakura and H. Kuroda, *Chem. Phys.*, 1984, **91**, 249; (*e*) J. E. Penner-Hahn, M. Benfatto, B. Hedman, T. Takahashi, S. Doniach, J. T. Groves and K. O. Hodgson, *Inorg. Chem.*, 1986, **25**, 2255.

16 T. Matsushita and R. P. Phizackerley, *Jpn. J. Appl. Phys.*, 1981, **20** 2223; R. P. Phizackerley, Z. U. Rek, G. B. Stephenson, S. D. Conradson, K. O. Hodgson, T. Matsushita and H. Oyanagi, *J. Appl. Crystallogr.*, 1983, **16**, 220.

17 (*a*) A. M. Flank, A. Fontaine, A. Jucha, M. Lemonnier, D. Raoux and C. Williams, *Nucl. Instrum. Methods*, 1983, **208**, 651; (*b*) E. Dartyge, C. Depautex, J. M. Dubuisson, A. Fontaine, A. Jucha, P. Leboucher and G. Tourillon, *Nucl. Inst. Methods*, 1986, **A 246**, 452.

18 EXAFS and Near Edge Structure IV, Fontevraud, 7 11th July, 1986, *J. Phys. (Les Ulis, Fr.)*, 1986, **47-C8**, 649.

19 L. Ricard, J. Fischer, R. Weiss and M. Momenteau, *Nouv. J. Chim.*, 1984, **8**, 649.

20 (*a*) I. A. Cohen, *J. Am. Chem. Soc.*, 1969, **91**, 1980; (*b*) A. B. Hoffmann, D. M. Collins, V. W. Day, E. B. Fleischer, T. S. Srivastava and J. L. Hoard, *J. Am. Chem. Soc.*, 1972, **94**, 3620; (*c*) J. T. Landram, D. Grimmett, K. J. Haller, W. A. Scheidt and C. A. Reed, *J. Am. Chem. Soc.*, 1981, **103**, 2640; (*d*) K. M. Kadish, G. Larson, D. Lexa and M. Momenteau, *J. Am. Chem. Soc.*, 1975, **97**, 282.

21 A. Fontaine, E. Dartyge, A. Jucha and G. Tourillon, *Nucl. Instrum. Methods*, 1987, **A 253**, 519; H. Tolentino, E. Dartyge, A. Fontaine and G. Tourillon, *J. Appl. Crystallogr.*, 1988, **21**, 15.

22 A. Michalowicz, J. Huet and A. Gaudemer, *Nouv. J. Chim.*, 1982, **6**, 79; M. Verdaguer, A. Michalowicz, J. J. Girerd, N. Alberding and O. Kahn, *Inorg. Chem.*, 1980, **19**, 3271; A. Michalowicz, M. Verdaguer, Y. Mathey and R. Clement, *Top. Curr. Chem.*, 1988, **145**, 107.
23 F. James and M. Roas, MINUIT, CERN Computing Center, Program Library, CERN/DD, internal report 75/20, 1976.
24 B. K. Teo and P. A. Lee, *J. Am. Chem. Soc.*, 1979, **101**, 2815.
25 G. Beni and P. A. Lee, *Phys. Rev. B*, 1977, **15**, 2862.
26 R. A. Bair and W. A. Goddard, *Phys. Rev. B*, 1980, **22**, 2767.
27 W. R. Scheidt, I. A. Cohen and M. E. Kastner, *Biochemistry*, 1979, 3546.
28 C. A. Reed, T. Mashiko, S. P. Bentley, M. E. Kastner, W. R. Scheidt, K. Spartalian and G. Lang, *J. Am. Chem. Soc.*, 1979, **101**, 2948.
29 J. P. Collman, R. R. Gagne, C. A. Reed, W. T. Robinson and G. A. Rodley, *Proc. Natl. Acad. Sci. USA*, 1974, **71**, 1326; G. B. Jameson, G. A. Rodley, W. T. Robinson, R. P. Gagne, C. A. Reed and J. P. Collman, *Inorg. Chem.*, 1978, **17**, 850.
30 G. B. Jameso, F. S. Molinaro, J. A. Ibers, J. P. Collman, J. I. Brauman, E. Rose and K. S. Suslick, *J. Am. Chem. Soc.*, 1978, **100**, 6769; 1980, **102**, 3224.
31 (*a*) W. R. Scheidt and M. Gouterman, in *Iron Porphyrins*, eds. A. B. P. Lever and H. B. Gray, Addison-Wesley, Reading, 1983, Part 1, p. 89; (*b*) A. B. Hoffman, D. H. Collins, V. W. Day, E. B. Fleischer, T. S. Srivastava and J. L. Hoard, *J. Am. Chem. Soc.*, 1972, **94**, 3620.
32 A. L. Roe, D. J. Schneider, R. J. Mayer, J. W. Pyrz, J. Windom and L. Que, *J. Am. Chem. Soc.*, 1984, **106**, 1676.
33 (*a*) C. Cartier, P. Thuery, M. Verdaguer, J. Zarembowitch and A. Michalowicz, *J. Phys.* (*Les Ulis, Fr.*), 1986, **47–C8**, 563; (*b*) C. Roux, J. Zarembowitch, M. Verdaguer, J. P. Itié, E. Dartyge, A. Fontaine and H. Tolentino, *Inorg. Chem.*, 1991, **30**, 3174.
34 G. Van der Laan, B. T. Thole, A. Sawatsky and M. Verdaguer, *Phys. Rev. B*, 1988, **37**, 6787.
35 G. Calas and J. Petiau, *Solid State Commun.*, 1983, **48**, 625.
36 C. Cartier, V. Briois, M. Maillard, M. Momenteau, E. Dartyge, A. Fontaine, G. Tourillon and M. Verdaguer, 1989, **86**, 1623.
37 C. Cartier, H. Homborg and M. Verdaguer, unpublished work.
38 C. E. Moore, *Atomic Energy Levels*, National Bureau of Standards, Washington D.C., 1971, vol. 2.
39 E. I. Solomon, personal communication.
40 G. Krill, *J. Phys.* (*Les Ulis, Fr.*), 1986, **47-C8**, 907 and refs. therein.
41 I. P. Gerothanassis, M. Momenteau and B. Loock, *J. Am. Chem. Soc.*, 1989, **111**, 7006.

Received 5*th August* 1991; *Paper* 1/04066I